Pathology (April 2024) **56(3)**, pp. 343–356

ANATOMICAL PATHOLOGY

Sarco/endoplasmic reticulum calcium ATPase 3 (SERCA3) expression in gastrointestinal stromal tumours

Homa Adle-Biassette[1,2], Riccardo Ricci[3,4], Antoine Martin[5,6], Maurizio Martini[7], Gloria Ravegnini[8], Rachid Kaci[1], Pascal Gélébart[9], Brigitte Poirot[10], Zsuzsanna Sándor[11], Jacqueline Lehman-Che[10,12,13], Erika Tóth[11], Bela Papp[12,13,14]

[1]*Service d'Anatomie et Cytologie Pathologiques, Hôpital Lariboisière, and Assistance Publique-Hôpitaux de Paris, Université de Paris, Paris, France;* [2]*INSERM NeuroDiderot, DMU DREAM, France;* [3]*Department of Pathology, Università Cattolica del Sacro Cuore, Rome, Italy;* [4]*UOC di Anatomia Patologica, Fondazione Policlinico Universitario 'A. Gemelli' IRCCS, Rome, Italy;* [5]*Service d'Anatomie et Cytologie Pathologiques, Hôpital Avicenne, Assistance Publique-Hôpitaux de Paris, Paris, France;* [6]*Inserm UMR U978, Université Sorbonne Paris Nord, Alliance Sorbonne Paris Cité, Labex Inflamex, Bobigny, France;* [7]*Dipartimento di patologia umana dell'adulto e dell'età evolutiva 'Gaetano Barresi' Azienda Ospedaliera Universitaria Policlinico 'G. Martino', Messina, Italy;* [8]*Department of Pharmacy and Biotechnology (FaBit), University of Bologna, Bologna, Italy;* [9]*Department of Clinical Science, University of Bergen, Bergen, Norway;* [10]*Molecular Oncology Unit, Hôpital Saint-Louis, Assistance Publique-Hôpitaux de Paris, Paris, France;* [11]*Department of Pathology, National Institute of Oncology, Budapest, Hungary;* [12]*INSERM UMR U976, Hôpital Saint-Louis, Paris, France;* [13]*Institut de Recherche Saint-Louis, Université de Paris, France;* [14]*CEA, DRF-Institut Francois Jacob, Department of Hemato-Immunology Research, Hôpital Saint-Louis, Paris, France*

Summary

Accurate characterisation of gastrointestinal stromal tumours (GIST) is important for prognosis and the choice of targeted therapies. Histologically the diagnosis relies on positive immunostaining of tumours for KIT (CD117) and DOG1. Here we report that GISTs also abundantly express the type 3 Sarco/Endoplasmic Reticulum Calcium ATPase (SERCA3). SERCA enzymes transport calcium ions from the cytosol into the endoplasmic reticulum and play an important role in regulating the intensity and the periodicity of calcium-induced cell activation. GISTs from various localisations, histological and molecular subtypes or risk categories were intensely immunopositive for SERCA3 with the exception of *PDGFRA*-mutated cases where expression was high or moderate. Strong SERCA3 expression was observed also in normal and hyperplastic interstitial cells of Cajal. Decreased SERCA3 expression in GIST was exceptionally observed in a zonal pattern, where CD117 staining was similarly decreased, reflecting clonal heterogeneity. In contrast to GIST, SERCA3 immunostaining of spindle cell tumours and other gastrointestinal tumours resembling GIST was negative or weak. In conclusion, SERCA3 immunohistochemistry may be useful for the diagnosis of GIST with high confidence, when used as a third marker in parallel with KIT and DOG1. Moreover, SERCA3 immunopositivity may be particularly helpful in cases with negative or weak KIT or DOG1 staining, a situation that may be encountered *de novo*, or during the spontaneous or therapy-induced clonal evolution of GIST.

Key words: Gastrointestinal stromal tumour; sarco/endoplasmic reticulum calcium ATPase; endoplasmic reticulum; calcium; interstitial cells of Cajal; immunohistochemistry; marker.

Received 24 July, accepted 18 October 2023
Available online 6 December 2023

INTRODUCTION

Gastrointestinal stromal tumours[1] (GISTs) are the most frequent mesenchymal neoplasms of the gastrointestinal system with malignant potential.[2] GISTs derive from interstitial cells of Cajal (ICCs) of the gastrointestinal tract that act as a pacemaker for stomach and intestine motility.[2] GISTs can be stratified according to various criteria such as histological appearance (fusiform, epithelioid or mixed morphology), localisation in the gastrointestinal tract, mitotic activity and size at diagnosis, and these parameters are useful for estimating the risk of malignant behaviour of the tumours.[3] Most often, the molecular oncogenesis of GIST involves mutations in the *KIT* (80–85% of cases; exons 11, 9, 13 and 17) or the *PDGFRA* (5–10% of cases; exons 12, 14 and 18) proto-oncogenes, leading to enhanced tyrosine kinase activity of the mutated oncoproteins.[4,5] Because the tyrosine kinase activity of several types of mutated KIT and PDGFRA enzymes can be inhibited by imatinib (Gleevec/Glivec) and related inhibitors, mutational analysis can be useful before starting treatment in GIST.[6–8] In tumours in which *KIT* or *PDGFRA* mutations cannot be found, mutations in other oncogenes and tumour suppressor genes, such as *BRAF* or *NF1*, have been reported.[9] In addition, GISTs

Print ISSN 0031-3025/Online ISSN 1465-3931
DOI: https://doi.org/10.1016/j.pathol.2023.10.012

in which the expression of the mitochondrial succinate dehydrogenase complex (SDH) is deficient due to mutations or epigenetic mechanisms have also been reported.[10–13] Familial GISTs have been observed in the context of germline mutations of the *KIT*, *PDGFRA* and *BRAF* genes, as well as in pedigrees with unknown mutations,[14] and can be preceded by Cajal cell hyperplasia, an excessive, polyclonal accumulation of normally located Cajal cells in the myenteric plexus.[15–17] Cases of GISTs for which the underlying molecular oncogenic mechanisms have not been identified are also known.[5]

Sarco/endoplasmic reticulum calcium-transporting ATPases (SERCA enzymes) are expressed in the endoplasmic reticulum (ER) membrane and carry out ATP-dependent active transport of calcium ions from the cytosol into the ER lumen.[18] SERCA-dependent calcium transport generates a several thousand-fold calcium ion concentration gradient between the cytosol (low nanomolar) and the ER lumen (high micromolar). Release of calcium from the ER into the cytosol through calcium channels such as the inositol-1,4,5-*tris*phosphate receptor, is a key element of calcium-dependent cell activation.[19,20] Because the overall displacement of calcium between the cytosol and the ER lumen as well as the dynamics of cytosolic calcium oscillations are determined by the net balance of SERCA and ER calcium channel activity, SERCA activity constitutes an essential and unique control mechanism of calcium-dependent cell activation.[21] SERCA proteins are coded by three genes (*ATP2A1, 2* and *3*) that by alternative splicing give rise to several SERCA protein isoforms.[22,23] SERCA1 is expressed in skeletal muscle, whereas SERCA2a is found in cardiomyocytes, and SERCA2b is expressed ubiquitously in non-muscle cells. In selected cell types such as Purkinje neurons, the choroid plexus epithelium, β-cells of pancreatic islets of Langerhans, endothelial cells, various cell types of haematological origin or gastric, colic, bronchial and mammary epithelium, SERCA2b is co-expressed with the SERCA3 isoenzyme.[24–35] Because the calcium affinity of SERCA3 is inferior to that of SERCA2b, their simultaneous

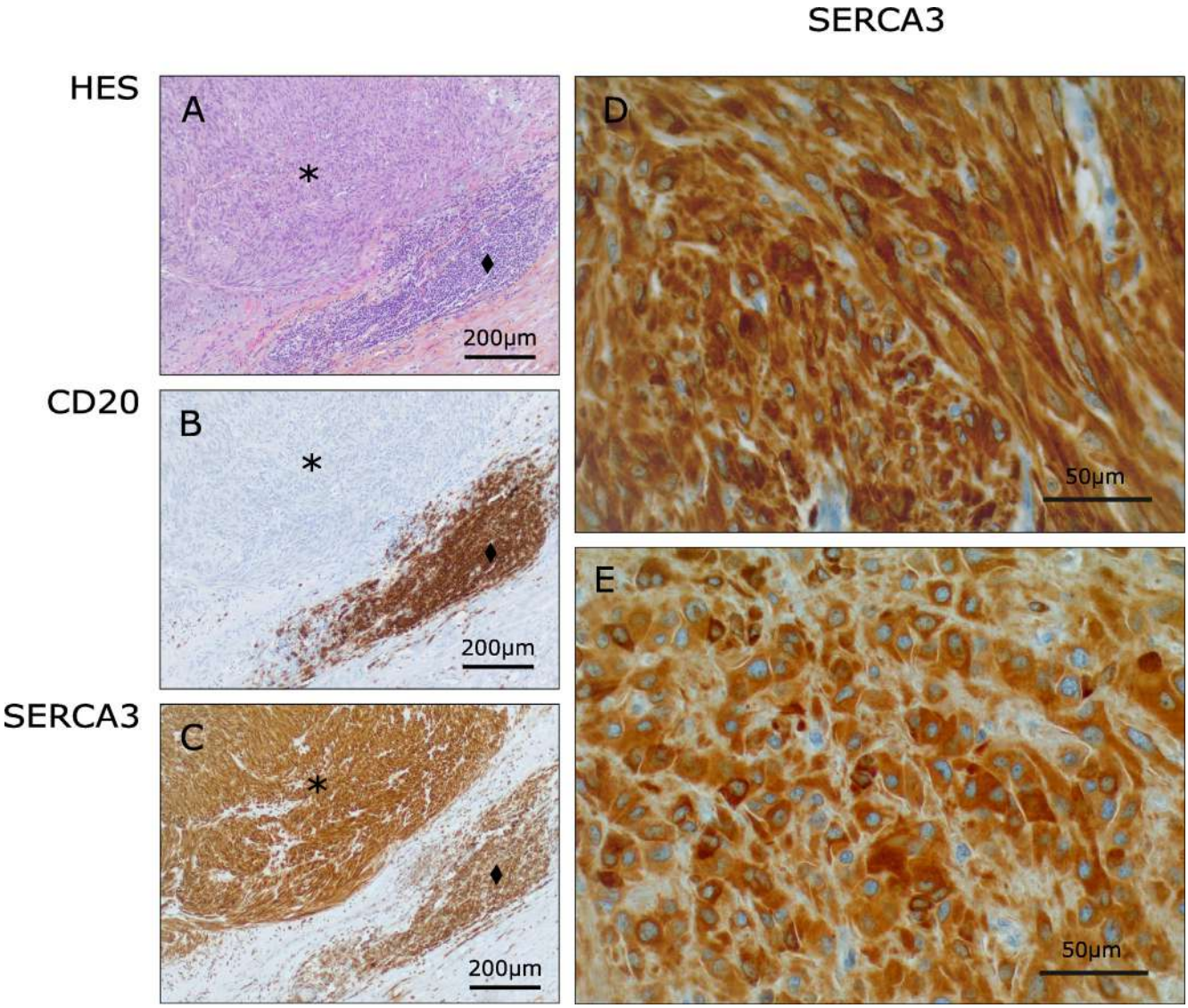

Fig. 1 Immunohistochemical labelling for SERCA3 protein in gastrointestinal stromal tumours (GIST). (A) Hematoxilin-eosin-saffron (HES) staining of GIST tissue containing tumour cells (*) and adjacent lymphocytes (◆). (B) Immunohistochemical staining with an anti-CD20 mouse monoclonal antibody (IgG2a, κ) used as isotype control showing lymphocytes, but not the tumour cells. (C) Immunohistochemical staining with the 2H3 anti-SERCA3 antibody labelling the tumour cells and the lymphocytes. (D,E) SERCA3 immunostaining in a fusiform (D) and an epithelioid (E) GIST.

expression is thought to confer unique calcium transport characteristics to the ER in these cell types, affecting the initiation of calcium signals and the spatiotemporal characteristics of cytosolic calcium oscillations required for specialised cellular functions.[21,36,37]

The immunohistochemical identification of GISTs is currently based on positive staining for CD117 (KIT, stem cell factor receptor) or DOG1 (Detected on GIST-1; anoctamin-1).[38–43] While most other histologically similar tumours of the gastrointestinal tract are negative, GISTs usually stain positively for these markers.[38–42] However, in some GIST-type tumours staining intensity may be low, and GISTs negative for either marker may also be encountered.[39,44–49] In addition, CD117 or DOG1 staining can be observed in non-GIST tumours as well.[39,43,50–53] Therefore, there is a need to further enhance the reliability of the immunohistochemical identification of GIST. In this work, SERCA3 expression was investigated by immunohistochemistry in normal and hyperplastic ICCs and in GISTs, and expression was compared to histologically similar non-GIST tumours of the gastrointestinal tract. The results indicate that SERCA3 may represent a new biomarker for the diagnosis of GIST and contribute to the better understanding of ICC and GIST calcium homeostasis and signalling.

MATERIALS AND METHODS

Samples

A total of 239 GIST tissue samples obtained from 138 individual cases defined according to the WHO Classification of Tumours, Digestive System Tumours, 5th edition,[54] and 63 non-GIST sarcomas were investigated. Risk classification of GIST was performed according to Miettinen *et al.*[3] Non-GIST tumours investigated in this study that resemble GIST histologically [23 leiomyomas, 6 leiomyosarcomas, 5 schwannomas and a malignant peripheral nerve sheath tumour, 3 cases of fibromatosis and a solitary fibrous tumour, 12 liposarcomas, 4 Kaposi sarcomas, a rhabdomyosarcoma, an angiosarcoma, a low-grade fibromyxoid sarcoma, a high-grade sclerosing epithelioid fibrosarcoma and 4 fibrosarcomas not otherwise specified (NOS)] were identified by standard histological, immunohistochemical and molecular biological methods. Archival formalin-fixed, paraffin-embedded (FFPE) tumour specimens were collected anonymously following ethical approval (CPP IDF4 N°2013-36NI, UCSC9421/18-15338/18-ID1969).

Immunohistochemistry

Immunohistochemical staining with the 2H3 mouse monoclonal anti-SERCA3 antibody (IgG2a, kappa, H00000489-MO1; Abnova, Taiwan) was performed on deparaffinised 5 µm thick sections using an indirect avidin-biotin-peroxidase method and 3,3′diaminobenzidine as chromogen, using the Benchmark automated immunostainer system (Ventana Medical Systems, France) as described previously.[25] Endogenous peroxidase activity was inhibited by incubation with 3% H_2O_2 in phosphate buffered saline for 10 min. Antigen retrieval was carried out using the Ventana CC1 *tris*-hydroxymethyl-aminoethane-based cell conditioning solution at 95–100°C for 30 min. Incubation with the SERCA3-specific primary antibody dissolved at 1.2 µg/mL in DakoReal antibody diluting reagent (Agilent, Singapore) was performed at 37°C for 30 min, and labelling was revealed using the Ventana *i*VIEW DAB Detection Kit with copper enhancement, according to the instructions of the manufacturer. Slides were counterstained with haematoxylin and bluing reagent (Ventana). SERCA3 staining was evaluated semi-quantitatively using a four-tiered scoring system (0–3+), and arteriolar endothelial cells and lymphocytes served as internal positive controls for SERCA3 staining.

In control experiments, staining was performed in identical conditions with an isotype-matched irrelevant antibody (Dako anti-CD20cy, clone L26), and this gave no staining on tumour tissue, while a strong positive staining was obtained on B-lymphocytes occasionally present in sections.

Although CD117 (KIT) and/or DOG1 (anoctamin-1) staining had already been carried out in the context of the initial diagnostic workup of the tumours, CD117 and DOG1 staining was repeated for all GIST specimens in this study with the Dako A4502 rabbit polyclonal (33 µg/mL), and the K9 (NCL-L-DOG-1, 70 µg/mL; Novocastra, Leica Biosystems, USA) mouse monoclonal antibodies, respectively, using a Benchmark automated immunostainer system (Ventana Medical Systems) according to the instructions of the manufacturers. Staining for SERCA3, CD117 and DOG1, as well as hematoxylin-eosin-saffron (HES) staining were performed on serial sections.

SDHB immunohistochemical staining was performed on all KIT and PDGFRA wild-type cases. Mouse monoclonal antibody to SDHB 21A11AE7 (1:1000; Abcam, USA) was used, and the Bond-Max autostainer (Leica Microsystems, USA) was employed using the Bond-Max avidin biotin-free polymer-based detection system and diaminobenzidine as the chromogen. Prior to staining, heat-induced epitope retrieval was carried out with the Leica alkaline antigen retrieval solution. Only slides with positive internal control (smooth muscle, endothelial, epithelial, or lymphoid cells) were considered for analysis. Photomicrographs were obtained using a AxioScope.A1 microscope and the AxioVision 4.8.2 image acquisition software (Zeiss, Germany).

Molecular biology

Mutational analysis was performed either by next generation sequencing (NGS) or polymerase chain reaction (PCR) amplification and sequencing of individual target genes. For NGS, DNA was extracted from selected tumour areas of FFPE specimens containing more than 30% tumour cells, using the Maxwell FFPE Plus DNA Kit (Promega, USA) on a Maxwell RSC (Promega). Mutational status of *c-KIT* (exons 8-11, 13, 17, 18; NM_000222) and PDGFRA (exons 12, 14, 18; NM_006206) was analysed with the Solid Tumour Solution capture-based target enrichment kit (Sophia Genetics, Switzerland) and sequenced on a MiSeq instrument on a v3 (2x300bp) flow cell (Illumina, USA). Bioinformatics data analysis was performed on SOPHiA DDM (Sophia Genetics) and pathogenic variants were reported, with a minimum of 1000X and 5% VAF.

DNA for PCR-based amplification and mutational analysis of individual target genes was obtained from FFPE tissues. Slides were cut from FFPE tissue blocks, treated twice with xylene, and washed with ethanol. Pathological areas (nearly 100% disease-specific tissue) were macro-dissected on slides. Mutational analysis was also performed in normal tissue (gastrointestinal wall layers, or lymph nodes). DNA was extracted using the QIAamp tissue mini kit (Qiagen, Germany). KIT exons 9, 11, 13, and 17 and PDGFRA exons 12, 14, and 18 were amplified using the primers and PCR conditions described earlier.[55–57] Briefly, DNA (100–200 ng) was amplified in a mixture containing 1xPCR buffer (20 mM TRIS, pH 8.3, 50 mM KCl, 1.5 mM $MgCl_2$), dNTPs (200 µM each), primers (20 pM each), and 0.5 U Platinum Taq polymerase (Invitrogen, Italy) in a 25 µL final volume. PCR conditions were: 8 min initial denaturation at 95°C, then 35 cycles at 95°C for 40s, 55°C for 40s, and 72°C for 40s. After visualisation on an agarose gel, PCR products were treated with ExoSAP-IT (USB Corp, USA) following the manufacturer's protocol, amplified with a BigDye Terminator version 3.1 cycle sequencing kit (Applied Biosystems, USA) using forward and reverse primers, and sequenced with an ABI PRISM 3100-Avant Genetic Analyzer (Applied Biosystems). Distilled water was included as the negative control. Genetic analysis of SDH subunits (A, B, C, D) was performed in immunohistochemically SDHB-negative cases. Each exon was amplified by PCR and sequenced, as previously reported.[58]

Statistical analysis

Non-parametric statistical analysis of SERCA3 staining intensities was performed with the unpaired Mann–Whitney U test using GraphPad Prism 5 (GraphPad Software, USA).

RESULTS

Labelling with the 2H3 monoclonal anti-SERCA3 antibody reproducibly gave a strong cytoplasmic staining in GIST cells as observed by light microscopy, in accordance with the localisation of SERCA3 protein in the endoplasmic reticulum (Fig. 1C–E). Staining was specific, as an isotype-matched anti-CD20 antibody gave no staining in the tumour cells, while recognising B-lymphocytes present in tissues (Fig. 1B).

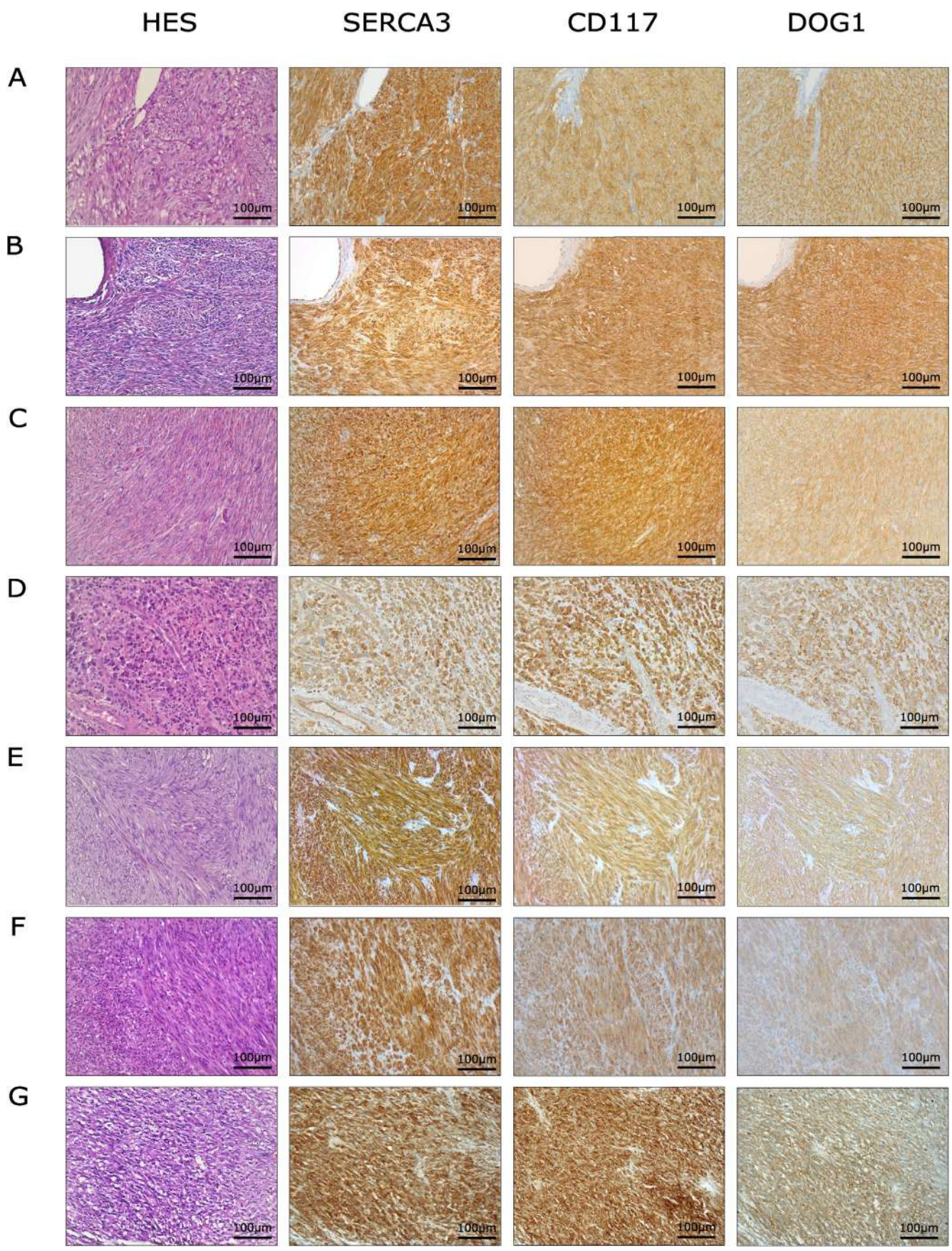

Fig. 2 SERCA3 immunohistochemical staining in *KIT*-mutated GISTs of various molecular and histological types, localisation and risk categories. Column 1, HES colouration; column 2, SERCA3; column 3, CD117 (KIT); column 4, DOG1 (anoctamin-1) immunostaining. (A) exon 9 c.1504_1509dup, p.A502_Y503dup, small intestine, low risk, spindle cell; (B) exon 9 c.1504_1509dup, p.A502_Y503dup, ileum, moderate risk, mixed morphology; (C) exon 11 c.1697T>G, p.V560G, colon, low risk, mixed morphology; (D) exon 11 c.1670G>C, p.W557S, liver metastasis from small intestinal primary, epithelioid; (E) exon 11 deletion, stomach, high risk, spindle cell; (F) KIT exon 11 c.1670_1717del, p.W557_P573del, stomach, very low risk, mixed morphology; (G) exon 13 c.1294A>G, p.K642E, stomach, high risk, spindle cell GIST.

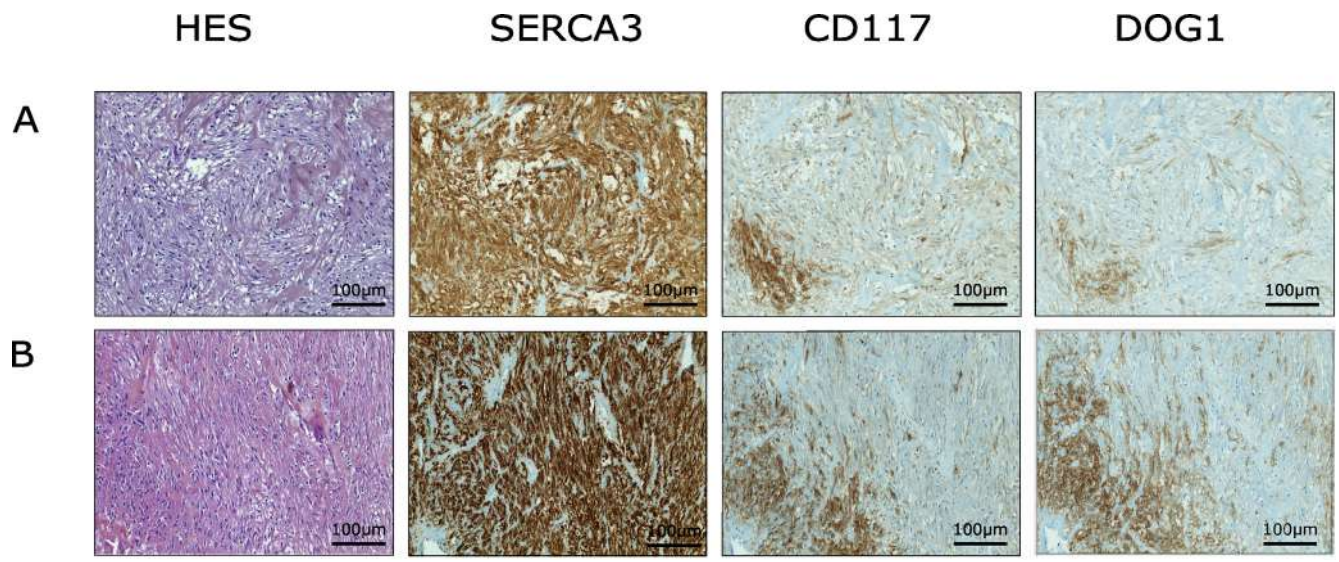

Fig. 3 Maintained SERCA3 expression in CD117-and DOG1-negative GIST cells. (A) Gastric, very low risk, KIT exon 11 mutated (c.1717_1755dup, p.P573_P585dup) GIST of mixed morphology; (B) duodenal, low risk, KIT exon 9 mutated (c.1509_1510ins, p.A502_Y503dup) GIST of fusiform morphology. Whereas in these tumours strongly KIT- and DOG1-positive regions, as well as regions in which CD117 and DOG1 labelling is very low or undetectable can be seen, SERCA3 labelling is strongly and homogenously positive, irrespective of the CD117 or DOG1 status of the tumour cells.

In accordance with previous studies,[27,29,31,34,35,59] SERCA3 staining with the 2H3 antibody could also be observed in lymphocytes, platelet aggregates, arteriolar endothelial cells, colonic crypts, and gastric surface epithelium when present in the samples.

As shown in Fig. 2, similarly to CD117 and DOG1, SERCA3 staining was strongly and consistently positive in *KIT* exon 9-, 11-, and 13-mutated tumours of gastric, small intestinal or colonic location, as well as in a liver metastasis. SERCA3 staining was observed independently of risk category very low, low, high, or metastatic in tumours of spindle cell, mixed or epithelioid morphology. Although CD117 and DOG1 staining was homogenously present in most tumours, in rare instances (2/138 tumours, 1.4%), staining for these markers was heterogeneous. In these tumours, large, homogenously CD117-and DOG1-negative or very weakly positive regions could be observed along with residual, strongly CD117- and DOG1-positive clusters of cells. However, despite the marked heterogeneity of CD117 and DOG1 labelling, SERCA3 staining in these tumours was strongly and homogenously positive (Fig. 3).

SERCA3 expression was observed also in *PDGFRA*-mutated GIST. As shown in Fig. 4, exon 18-, exon 12- or exon 14-mutated GISTs of spindle cell, epithelioid or mixed morphology, including very low to moderate to high risk and metastatic tumours all stained positive for SERCA3. Of note, the intensity of SERCA3 staining was more variable among *PDGFRA*-mutated, than among *KIT*-mutated tumours, as tumours of high, as well as moderate staining intensity could be observed.

SERCA3 immunostaining was strong in SDH-deficient stomach GIST (Fig. 5A–E), including *SDHA*-, *SDHB*- and *SDHC*-mutated tumours of epithelioid, mixed and plexiform morphology. SERCA3 expression could also be seen in Neurofibromin-1 (*NF1*)-mutated GIST (Fig. 5F). Wild-type tumours, defined by a wild-type sequence in *KIT* exons 9, 11, 13 and 17, *PDGFRA* exons 12, 14 and 18, *BRAF* exon 15 and *KRAS* exons 2 and 3 and SDHB immunohistochemical positivity (Fig. 6), gastric or duodenal location, of very low, low or moderate risk of mixed or fusiform morphology were also strongly positive for SERCA3 expression. A DOG1-negative malignant pericolic GIST with moderate SERCA3 staining was also encountered. This may be due to the possibility that the group of wild-type GIST is heterogeneous. SERCA3 staining could also be detected in residual viable GIST cells after imatinib treatment, as well as in ICCs present in a leiomyoma (not shown). In several instances, SERCA3 immunohistochemistry in GISTs gave stronger staining than DOG1 or CD117 (Fig. 2A,F, Fig. 5A,C,D, Fig. 6A,B).

Taken together, these observations indicate that SERCA3 expression is readily detected by immunohistochemistry in most GISTs. Uniformly strong and homogeneous SERCA3 expression could be observed consistently in most primary tumours of various molecular types (*i.e., KIT*-, *NF1*-mutated, SDH-deficient or wild-type), whereas expression in *PDGFRA*-mutated tumours was strong or moderate. Analysis of SERCA3 staining intensity did not disclose significant differences depending on risk category in GIST (Supplementary Fig. 1A, Appendix A). On the other hand, a decreasing trend from high to moderate intensity of SERCA3 staining could be observed in tumours of mixed and epithelioid morphology, when compared to fusiform tumours (Supplementary Fig. 1B, Appendix A). This is in accordance with observations in the literature,[60,61] as well as with our own data indicating that *PDGFRA*-mutated tumours usually display mixed or epithelioid morphology. A marginally significant, increasing trend of SERCA3 staining intensity observed between gastric and small intestinal tumours can also be attributed to this phenomenon, as statistical significance was abolished when *PDGFRA*-mutated gastric tumours were omitted from analysis (Supplementary Fig. 1C, Appendix A).

In most tumours (126/138 tumours investigated, 91.3%) SERCA3 expression was homogeneous. However, in a minority of tumours (12, 8.7%), the intensity of SERCA3 labelling displayed an obvious spatial heterogeneity, with clearly delineated boundaries. Fig. 7A, shows a high-risk, small intestinal wild-type tumour containing a clearly

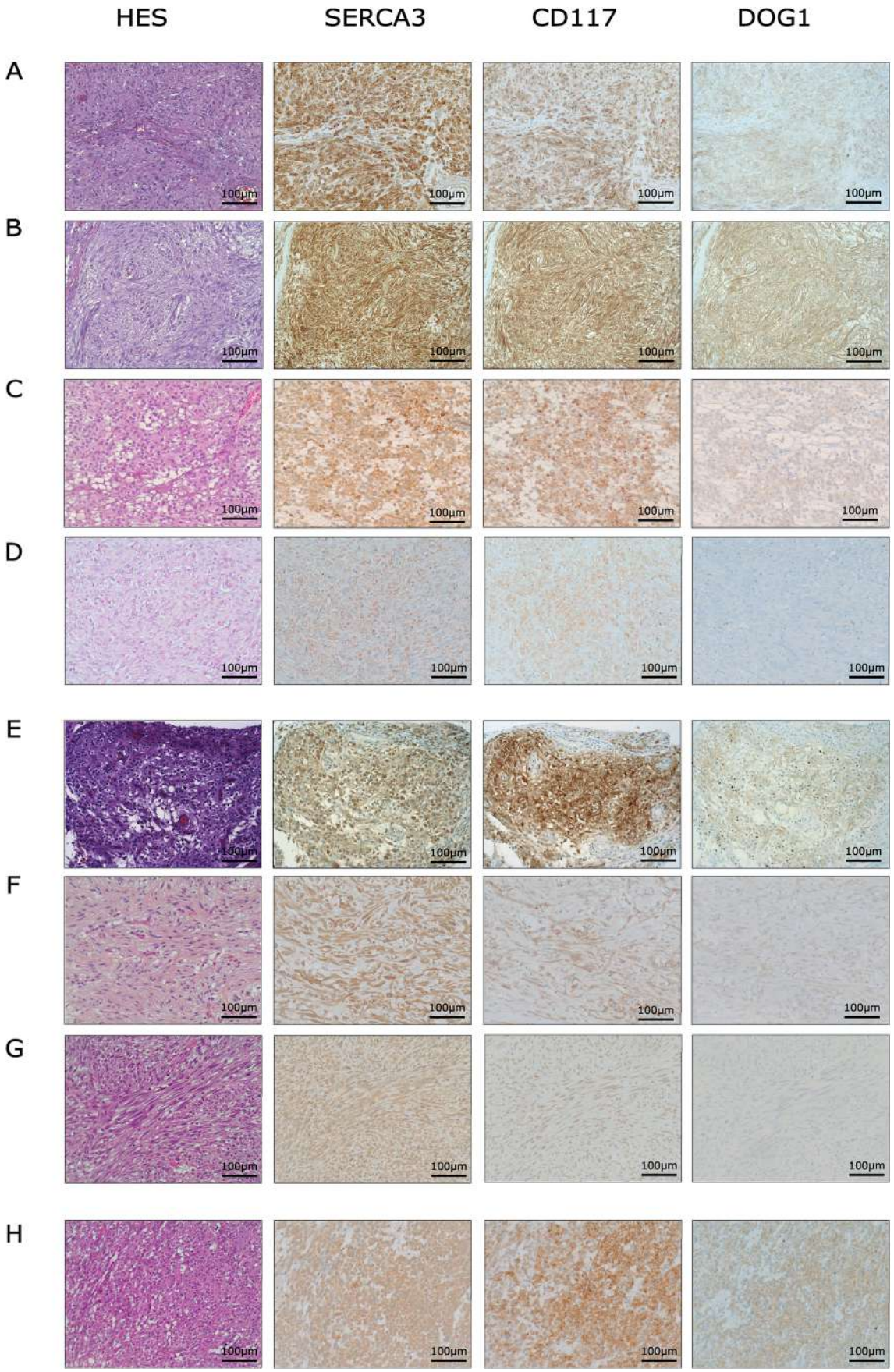

Fig. 4 SERCA3 immunohistochemical staining in *PDGFRA*-mutated GISTs of various molecular and histological types and risk categories. Column 1, HES colouration; column 2, SERCA3; column 3, CD117 (KIT); column 4, DOG1 (anoctamin-1) immunostaining. (A) exon 18 c.2527_2538del, p.T843_D846del, very low risk, epithelioid, gastric; (B) exon 18 c.2525A>T p.D842V, very low risk, spindle cell, gastric; (C) exon 18 c.2586A>T, p.D842V, high risk, epithelioid, gastric; (D) exon 18 c.2525A>T, p.D842V, moderate risk, mixed morphology, gastric; (E) exon 12 c.1682T>A, p.V561D very low risk epithelioid, gastric; (F) exon 12 c.1682T>A p.V561D, low risk, mixed morphology, gastric; (G) exon 12 c.1750_1759 tcaagatggg>ctcg, del p.S584_E587>LQ, spindle cell, peritoneal, malignant; (H) exon 14 c.1977C>G, p.N659K, moderate risk, epithelioid, gastric GIST.

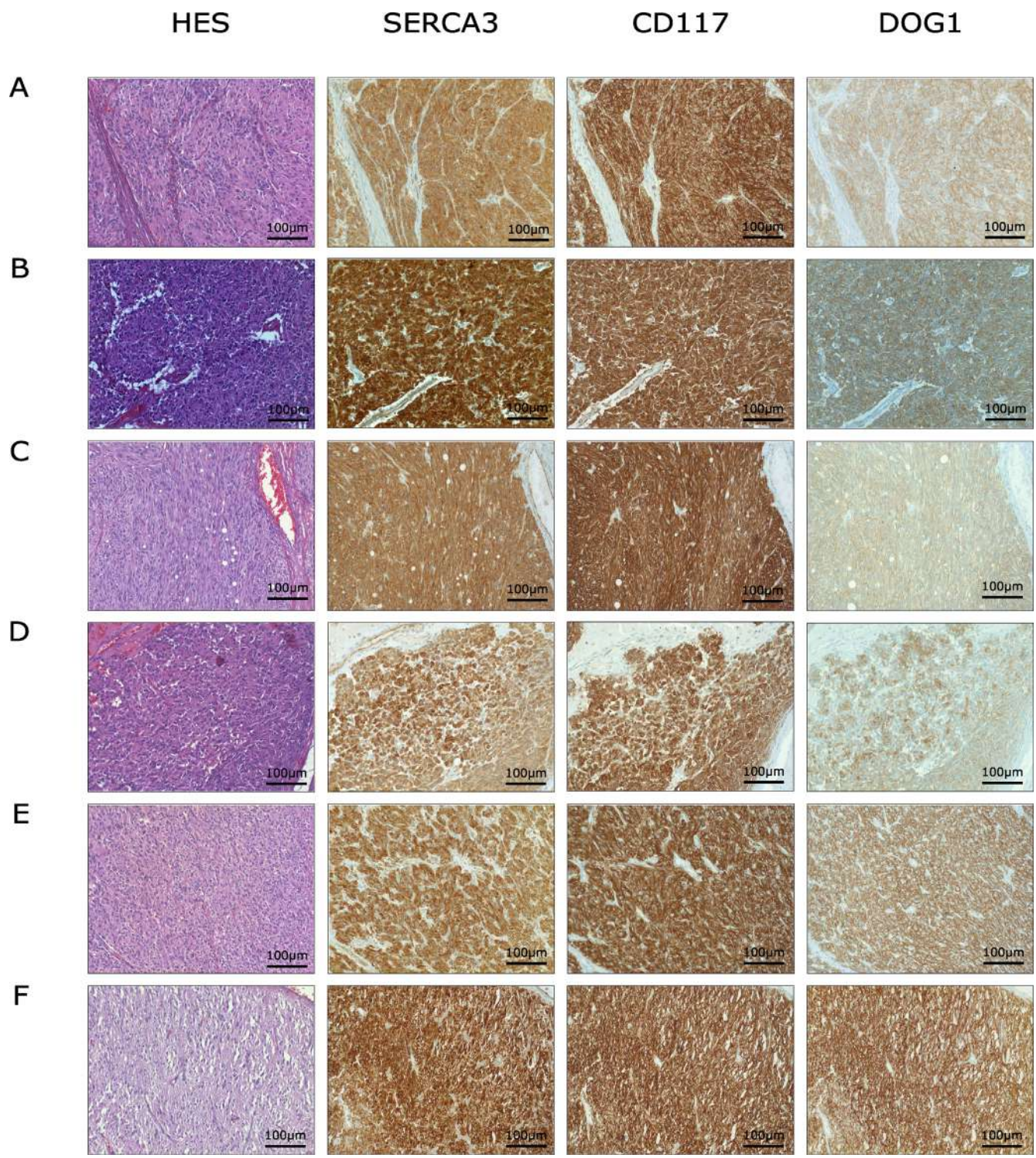

Fig. 5 SERCA3 immunohistochemical staining in SDH-deficient and NF1-mutated GISTs of various molecular and histological types. Column 1, HES colouration; column 2, SERCA3; column 3, CD117 (KIT); column 4, DOG1 (anoctamin-1) immunostaining. (A) SDHA exon 9 c.1255G>A, p.G419R heterozygous somatic mutation, gastric, epithelioid; (B) SDHA exon 1 c.26G>A, p.R9Q and exon 13 c.1729C>A, p.Q577K (heterozygous somatic mutation), gastric, mixed morphology; (C) SDHA exon 10 c.1394G>A, p.R465Q gastric, epithelioid; (D) SDHB exon 6 c.638T>G p.R465Q, homozygous somatic mutation, gastric, epithelioid; (E) SDHC exon 4 c.224G>A, p.G75D, gastric, epithelioid plexiform GIST. (F) NF1 one nucleotide insertion, frameshift c.3892_3893ins A, p.L1300fs*14, jejunum, fusiform.

demarcated region with decreased expression of both SERCA3 and KIT, but maintained levels of DOG1 protein. In a gastric *PDGFRA* exon 18 c.2525 A>T, p.D842V-mutant low risk GIST of mixed morphology, the loss of SERCA3 expression could be observed in two steps, in a 'nodule-in-nodule'-type pattern. As shown in Fig. 7C, whereas clear SERCA3 and DOG1 expression as well as weaker CD117 expression could be observed in the bulk tumour parenchyma, the expression of all three markers was decreased in an intermediary region (Fig. 7D, right), and lost in a central nodule (Fig. 7E). Interestingly, in both tumours, the loss of SERCA3 expression was associated with transition to a pure

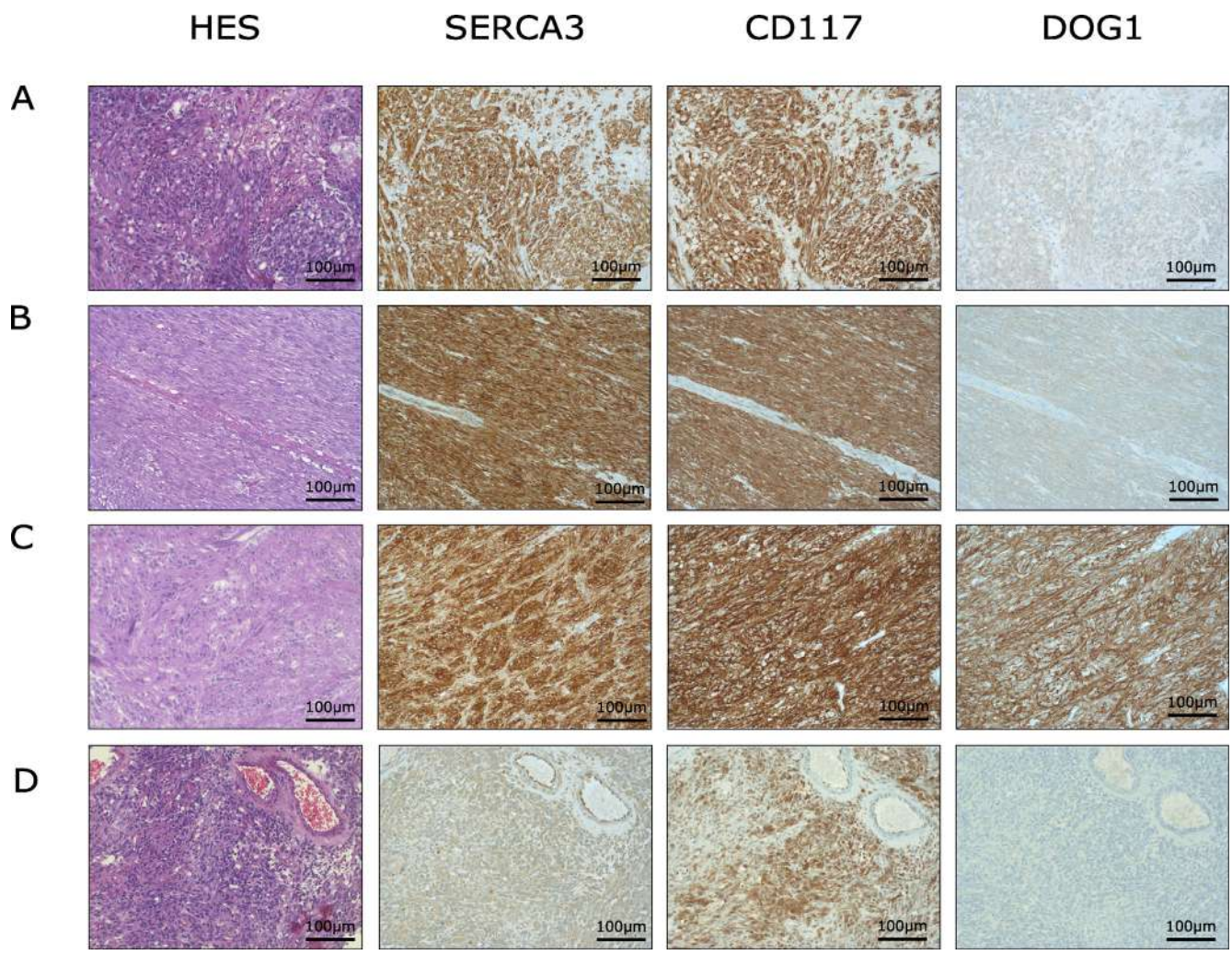

Fig. 6 SERCA3 immunohistochemical staining on wild-type GIST. Column 1, HES colouration; column 2, SERCA3; column 3, CD117 (KIT); column 4, DOG1 (anoctamin-1) immunostaining. (A) Gastric, mixed morphology, very low risk; (B) gastric, spindle cell, low risk; (C) duodenal, spindle cell, moderate risk; (D) pericolic, mixed morphology, metastatic GIST.

epithelioid morphology and increased cellularity as observed by higher nuclear density (Fig. 7B,E). These observations indicate that the loss of SERCA3 expression may be associated with intratumour clonal heterogeneity and possibly tumour progression, as has been previously described for the two other markers in GIST.[44–46,62–64]

As shown in Fig. 8, SERCA3 staining could also be observed in normal ICCs in the myenteric plexus (Fig. 8A), as well as in Cajal cell hyperplasia in type 1 neurofibromatosis (Fig. 8B), whereas ganglion cells and surrounding smooth muscle were negative, or gave only a very weak staining. This is in agreement with transcriptomic data indicating higher SERCA3 (*ATP2A3*) mRNA levels in mouse small intestinal ICCs, when compared with surrounding tissue.[65] The overall aspect of the distribution of the SERCA3 label was very similar to CD117 or DOG1, the two generally used markers of ICCs.

In contrast to GIST, other, histologically similar tumours of the gastrointestinal tract displayed weak or undetectable SERCA3 immunohistochemical labeling. As shown in Fig. 9, in tumours of smooth muscle or nerve sheath differentiation of gastric, small intestinal or colonic location, in fibroblastic lesions such as fibromatosis, solitary fibrous tumour, as well as in gastric or small intestinal Kaposi sarcoma or in poorly differentiated liposarcoma, SERCA3 labelling was weak or undetectable, and low grade fibromyxoid sarcoma displayed moderate staining. Thus, strong SERCA3 staining was not encountered in any of the non-GIST tumours investigated in this study, whereas positive internal controls such as vascular endothelial cells, lymphocytes, platelet aggregates or colonic epithelium were consistently positive. The intensity of SERCA3 expression in various molecular types of GIST as compared to non-GIST-type tumours as a group is summarised in Fig. 10.

DISCUSSION

SERCA enzymes transport calcium ions from the cytosol into the ER lumen by active, ATP-dependent ion transport, which constitutes the only known mechanism of calcium accumulation in this organelle. Calcium release from the ER back to the cytosol is the first step of calcium-dependent cell activation, making SERCA enzymes an indispensable component of calcium-dependent intracellular signaling. In addition, by re-sequestering calcium from the cytosol into the ER following cell activation, they contribute to the shaping of the spatiotemporal characteristics of oscillatory calcium signals, and to the termination of a calcium-dependent cell activation event.

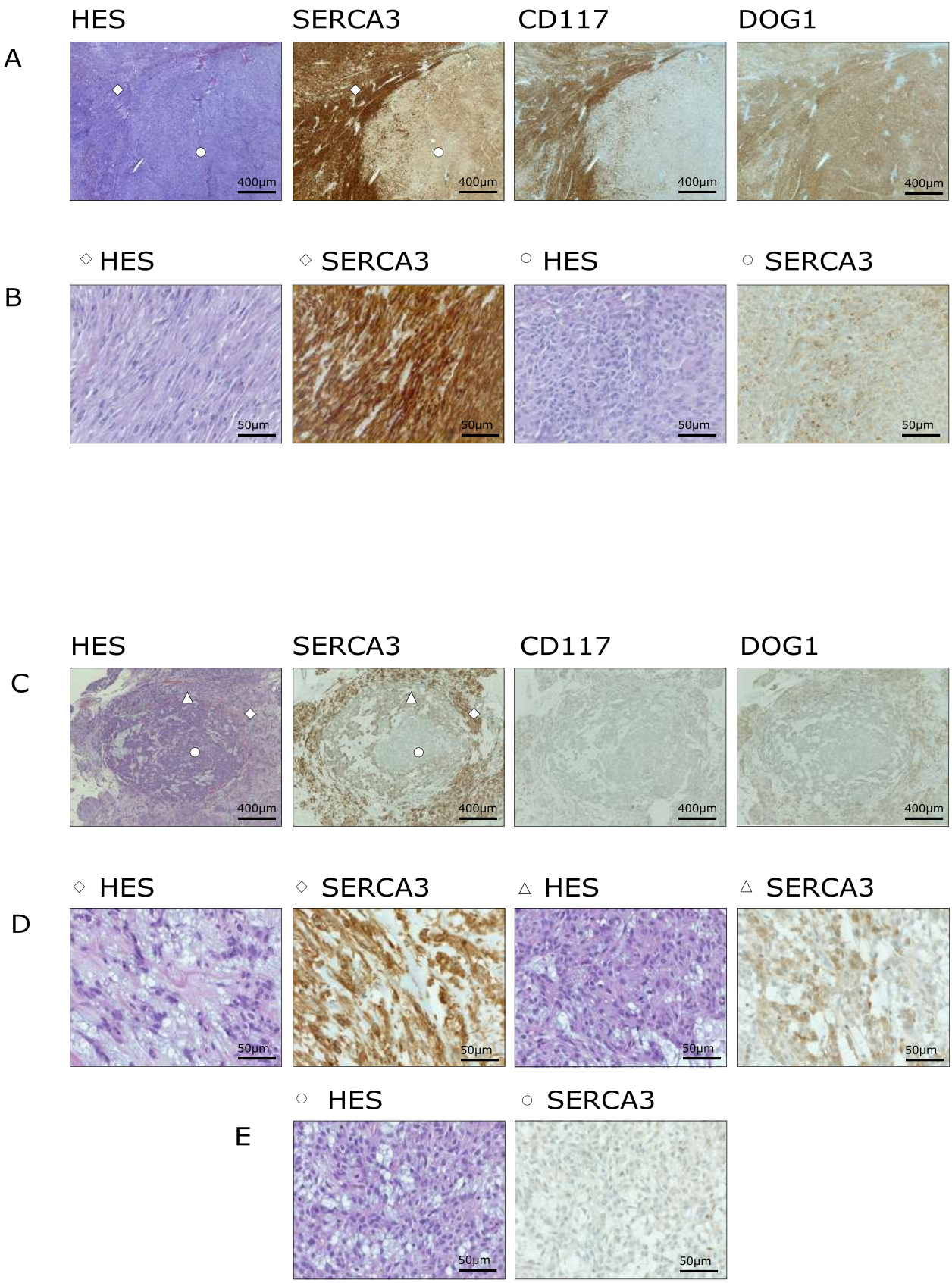

Fig. 7 Loss of SERCA3 expression in GIST. (A,B) A SERCA3^{low}, CD117^{low}, DOG1^{high} region (○) is observed in a SERCA3^{high}, CD117^{high}, DOG1^{high} (◊), KIT exon 9, 11, 13, 17, PDGFRA exon 12, 14, 18 wild-type small intestinal, high-risk GIST. (B) Whereas the SERCA3^{high} region (◊) of this tumour is of fusiform morphology, the SERCA3^{low} region (○) is of epithelioid morphology and displays increased cell density. (C–E) Loss of SERCA3 expression, in a 'nodule-in-nodule' manner, in a low risk, PDGFRA exon 18 c.2525A>T (p.D842V) gastric GIST of mixed morphology. (D,E) Whereas tumour cells on the periphery (◊) express SERCA3 abundantly, SERCA3 expression is decreased in an intermediate zone (Δ), and is lost in a central, epithelioid region (○) of increased cell density.

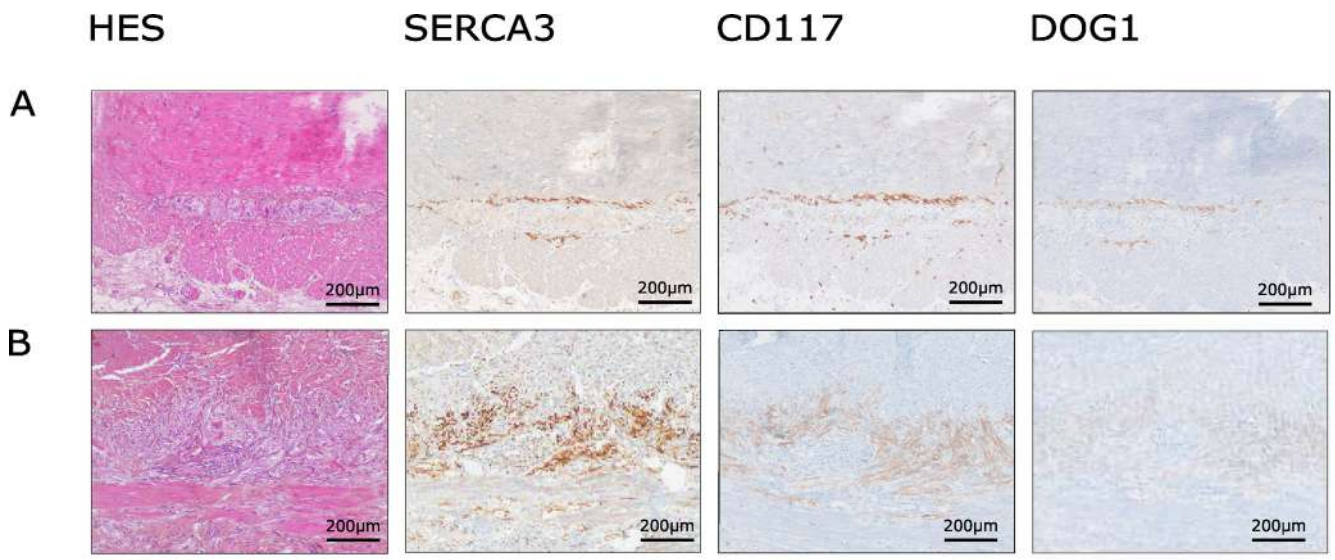

Fig. 8 SERCA3 expression in normal and hyperplastic interstitial cells of Cajal (ICCs). Column 1, HES colouration; column 2, SERCA3; column 3, CD117 (KIT); column 4, DOG1 (anoctamin-1) immunostaining. (A) Normal ICC in jejunal musculosa; (B) hyperplastic ICCs in the muscular layer of ileum in a case of type I neurofibromatosis and familial GIST.

Calcium signalling plays an important role in the induction and regulation of periodic electrical signals generated in ICCs, as well as in the transfer of these signals to surrounding smooth muscle.[66] Increased cytosolic calcium levels trigger the opening of calcium-activated ion channels located in the plasma membrane, including anoctamin-1, leading to trans-plasma membrane ion fluxes, depolarisation and pacemaker potentials that are propagated to gastrointestinal smooth muscle to induce peristalsis.[66–69] The release of calcium ions into the cytosol from the ER, followed by pool depletion-induced calcium influx (store-operated calcium entry, SOCE) strongly increase cytosolic calcium levels, and this is indispensable for the maintenance of pacemaker signals by ICCs.[68–76] The pacemaker activity of ICCs can be perturbed or abolished by the specific pharmacological inhibition of SERCA-dependent calcium transport.[68–76] Moreover, normal KIT or PDGFRA proteins, as well as their mutated forms found in GIST can induce calcium-dependent cell activation through phospholipase-C activation and consequent second messenger-induced calcium release from the ER.[20,77–80] Therefore, in addition to its involvement in pacemaker function, SERCA activity may contribute to regulate the proliferation of normal and hyperplastic ICCs, as well as of GIST.

The calcium affinity of SERCA3 (~1.2 μM) is significantly lower than that of the ubiquitous SERCA2b isoform (~0.2 μM).[35,37,81–83] Therefore, ER calcium release is counteracted more weakly by SERCA3 than by SERCA2b. SERCA3 thus being a less stringent calcium pump than SERCA2, it will tolerate greater calcium release events during cell activation than SERCA2b. Thus, calcium re-sequestration into SERCA3-associated intracellular calcium pools will begin later during a calcium activation event, and at higher cytosolic calcium levels, when compared to SERCA2b-associated pools.[21] Therefore, SERCA3 is well-adapted to regulate the initiation of calcium signals in specialised cell types with prominent calcium signalling. In accordance with this, abundant SERCA3 expression has already been described in platelets, mature T- and B-lymphocytes, and cerebellar Purkinje neurons,[27,31,32,34,84–86] cell types in which calcium activation is essential for the induction of specific effector functions. Moreover, in platelets it has been shown that the SERCA3-associated calcium pool is specifically involved in the initiation and initial amplification of intracellular calcium mobilisation, which is then followed by calcium release from SERCA2b-associated intracellular calcium pools.[87,88] Based on the abundant expression of SERCA3 in normal and hyperplastic ICCs presented in this work, it is tempting to hypothesise that SERCA3 expression is part of a specialised calcium homeostatic machinery present in ICCs, required for their formation and pacemaker function. Maintained SERCA3 expression in GIST suggests that this machinery may also be involved in GIST tumourigenesis. Similar to KIT, PDGFRA or anoctamin-1, expression of SERCA3 may be subsequently downregulated during the post-clonal evolution of tumours, where secondary oncogenic events render it superfluous.[44–46,62–64,89]

In contrast with GISTs, SERCA3 expression was low or negative in gastrointestinal leiomyomas and nerve sheath tumours, as well as in other, less frequent benign or malignant GIST histological mimics, such as various fibroblastic tumours, dedifferentiated liposarcoma, and leiomyosarcoma or Kaposi sarcoma. Our search in the Gene Expression Omnibus transcriptomic database[90,91] also indicates that, in an unrelated study,[92,93] SERCA3 expression was higher at the mRNA level in GISTs, when compared to pleomorphic and dedifferentiated liposarcomas, leiomyosarcoma, round cell and synovial sarcoma, as well as fibrosarcomas and tumours classified as malignant fibrous histiocytomas (Supplementary Fig. 2, Appendix A).

High SERCA3 expression in GISTs, when compared to low or absent expression in other, histologically similar mesenchymal tumours of the gastrointestinal tract, suggests that SERCA3 may be useful for the positive identification of GIST by immunohistochemistry, as strong SERCA3 staining in this setting indicates GIST with high confidence. When used as a third marker, strong positive SERCA3 labelling may further strengthen diagnosis based on positive CD117

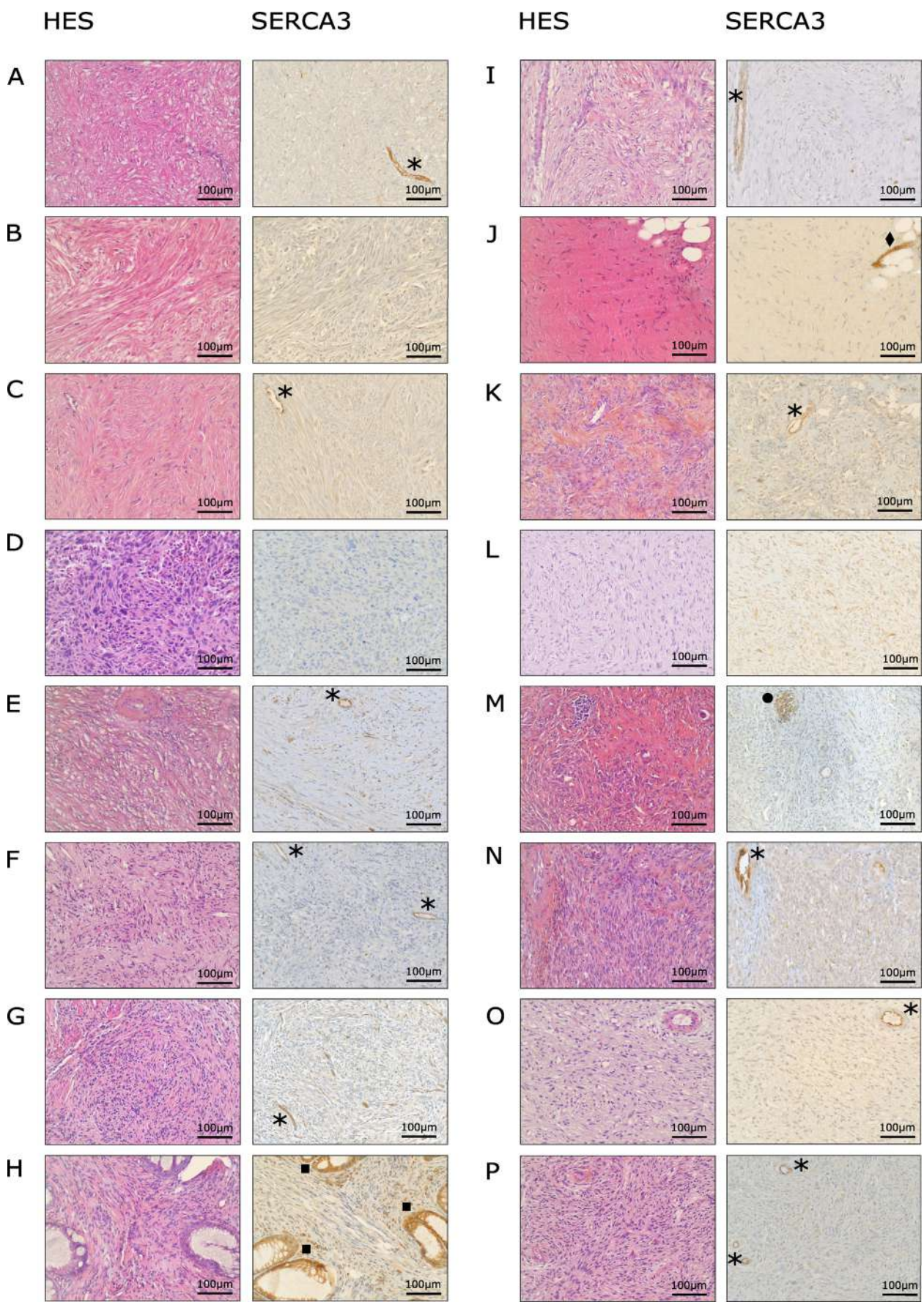

Fig. 9 Lack of SERCA3 expression in various tumours histologically similar to GIST. Left columns, HES colouration; right columns, SERCA3 immunohistochemical staining. (A) Gastric leiomyoma; (B) small intestinal leiomyoma; (C) colic leiomyoma; (D) poorly differentiated colic leiomyosarcoma; (E) gastric schwannoma; (F) gastric neurinoma; (G) gastric schwannoma; (H) colic ganglioneuroma; (I) abdominal fibromatosis; (J) mesenterial fibromatosis; (K) solitary fibrous tumour, benign, liver; (L) low grade fibromyxoid sarcoma; (M) Kaposi sarcoma, gastric; (N) Kaposi sarcoma, small intestine; (O) poorly differentiated peritoneal liposarcoma; (P) poorly differentiated liposarcoma. Internal positive controls for SERCA3 staining: vascular endothelial cells (*), aggregated platelets, (◆); lymphocytes (●) and colonic crypt epithelial cells (■).

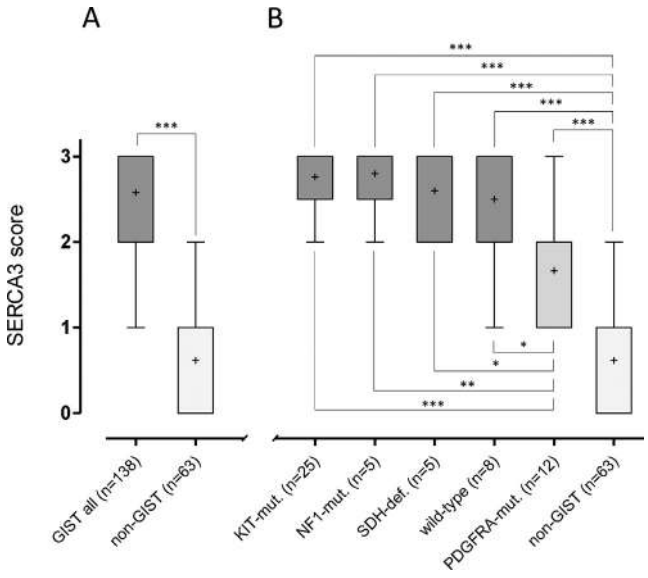

Fig. 10 Statistical analysis of SERCA3 expression in GIST compared to non-GIST tumours. (A) Comparison of SERCA3 expression in all investigated GIST-type tumours combined as a group, versus non-GIST tumours. (B) SERCA3 expression in various molecular types of GIST (*KIT*-mutated, *NF1*-mutated, SDH-deficient, wild-type and *PDGFRA*-mutated) compared to histologically similar, non-GIST tumours as a group. Box plot (box, interquartile range; whiskers, minimum/maximum; +, mean) with Mann–Whitney two-tailed unpaired test (*p<0.05, **p<0.01, ***p<0.0001).

and DOG1 staining. Moreover, SERCA3 positivity may be particularly helpful in cases when CD117 or DOG1 staining is weak or absent, a situation that may be encountered *de novo*, or during the spontaneous or therapy-induced clonal evolution of GIST.[44,45,62–64,94–96]

As a caveat, it should be noted that SERCA3 expression, although homogeneous in a given tumour, was more variable (*i.e.,* high or moderate) among *PDGFRA*-mutated GIST cases than in *KIT*-mutated tumours. This may be related to different KIT (CD117) or PDGFRA expression levels reported in various sub-populations of GIST precursor cells,[4,97–102] as well as to differences in PDGFRA- versus KIT-related downstream signalling mechanisms.[103,104]

Taken together, the observations presented in this work indicate that SERCA3 constitutes a new phenotypic marker of ICC, and that SERCA3 may be potentially useful for the identification of GISTs, as well as for the study of their cellular origin, clonal evolution, and dedifferentiation.

Acknowledgements: We would like to thank Prof Anne Lavergne-Slove, Dr David Garrick and Ms Katalin Varga for their support during this work. This work is dedicated to the memory of Lugosi Judit Papp Béláné.

Conflicts of interest and sources of funding: The authors state that there are no conflicts of interest to disclose. Institutional support from Inserm, France, is acknowledged.

APPENDIX A. SUPPLEMENTARY DATA

Supplementary data to this article can be found online at https://doi.org/10.1016/j.pathol.2023.10.012.

Address for correspondence: Dr Bela Papp, INSERM UMR U976, Institut de Recherche Saint-Louis, Hôpital Saint-Louis, 1, avenue Claude Vellefaux, 75475 Cedex 10, Paris, France. E-mails: belapapp2@yahoo.fr, bela.papp@inserm.fr

References

1. Kindblom LG, Remotti HE, Aldenborg F, Meis-Kindblom JM. Gastrointestinal pacemaker cell tumour (GIPACT): gastrointestinal stromal tumours show phenotypic characteristics of the interstitial cells of Cajal. *Am J Pathol* 1998; 152: 1259–69.
2. Blay JY, Kang YK, Nishida T, von Mehren M. Gastrointestinal stromal tumours. *Nat Rev Dis Primers* 2021; 7: 22.
3. Miettinen M, Lasota J. Gastrointestinal stromal tumours: pathology and prognosis at different sites. *Semin Diagn Pathol* 2006; 23: 70–83.
4. Dermawan JK, Rubin BP. Molecular pathogenesis of gastrointestinal stromal tumour: a paradigm for personalized medicine. *Annu Rev Pathol* 2022; 17: 323–44.
5. Brcic I, Argyropoulos A, Liegl-Atzwanger B. Update on molecular genetics of gastrointestinal stromal tumours. *Diagnostics (Basel)* 2021; 11: 194.
6. Klug LR, Khosroyani HM, Kent JD, Heinrich MC. New treatment strategies for advanced-stage gastrointestinal stromal tumours. *Nat Rev Clin Oncol* 2022; 19: 328–41.
7. Laurent M, Brahmi M, Dufresne A, *et al.* Adjuvant therapy with imatinib in gastrointestinal stromal tumours (GISTs)-review and perspectives. *Transl Gastroenterol Hepatol* 2019; 4: 24.
8. Pathania S, Pentikainen OT, Singh PK. A holistic view on c-Kit in cancer: structure, signaling, pathophysiology and its inhibitors. *Biochim Biophys Acta Rev Cancer* 2021; 1876: 188631.
9. Wada R, Arai H, Kure S, Peng WX, Naito Z. "Wild type" GIST: clinicopathological features and clinical practice. *Pathol Int* 2016; 66: 431–7.
10. Ibrahim A, Chopra S. Succinate dehydrogenase-deficient gastrointestinal stromal tumours. *Arch Pathol Lab Med* 2020; 144: 655–60.
11. Janeway KA, Kim SY, Lodish M, *et al.* Defects in succinate dehydrogenase in gastrointestinal stromal tumours lacking KIT and PDGFRA mutations. *Proc Natl Acad Sci USA* 2011; 108: 314–8.
12. Miettinen M, Lasota J. Succinate dehydrogenase deficient gastrointestinal stromal tumours (GISTs) - a review. *Int J Biochem Cell Biol* 2014; 53: 514–9.
13. Boikos SA, Stratakis CA. The genetic landscape of gastrointestinal stromal tumour lacking KIT and PDGFRA mutations. *Endocrine* 2014; 47: 401–8.
14. Ricci R. Syndromic gastrointestinal stromal tumours. *Hered Cancer Clin Pract* 2016; 14: 15.
15. Vale Rodrigues R, Santos F, Pereira da Silva J, *et al.* A case of multiple gastrointestinal stromal tumours caused by a germline KIT gene mutation (p.Leu576Pro). *Fam Cancer* 2017; 16: 267–70.
16. Nishida T, Hirota S, Taniguchi M, *et al.* Familial gastrointestinal stromal tumours with germline mutation of the KIT gene. *Nat Genet* 1998; 19: 323–4.
17. Chen H, Hirota S, Isozaki K, *et al.* Polyclonal nature of diffuse proliferation of interstitial cells of Cajal in patients with familial and multiple gastrointestinal stromal tumours. *Gut* 2002; 51: 793–6.
18. Chen J, Sitsel A, Benoy V, Sepulveda MR, Vangheluwe P. Primary active Ca(2+) transport systems in health and disease. *Cold Spring Harb Perspect Biol* 2020; 12: a035113.
19. Woll KA, Van Petegem F. Calcium-release channels: structure and function of IP3 receptors and ryanodine receptors. *Physiol Rev* 2022; 102: 209–68.
20. Berridge MJ. The inositol trisphosphate/calcium signaling pathway in health and disease. *Physiol Rev* 2016; 96: 1261–96.
21. Papp B, Launay S, Gélébart P, *et al.* Endoplasmic reticulum calcium pumps and tumour cell differentiation. *Int J Mol Sci* 2020; 21: 3351.
22. Vangheluwe P, Sepulveda MR, Missiaen L, Raeymaekers L, Wuytack F, Vanoevelen J. Intracellular Ca^{2+}- and Mn^{2+}-transport ATPases. *Chem Rev* 2009; 109: 4733–59.
23. Bobe R, Bredoux R, Corvazier E, *et al.* How many Ca(2)+ATPase isoforms are expressed in a cell type? A growing family of membrane proteins illustrated by studies in platelets. *Platelets* 2005; 16: 133–50.
24. Ait-Ghezali L, Arbabian A, Jeibmann A, *et al.* Loss of endoplasmic reticulum calcium pump expression in choroid plexus tumours. *Neuropathol Appl Neurobiol* 2014; 40: 726–35.

25. Arbabian A, Brouland JP, Apàti A, *et al*. Modulation of endoplasmic reticulum calcium pump expression during lung cancer cell differentiation. *FEBS J* 2013; 280: 5408–18.
26. Papp B, Brouland JP. Altered endoplasmic reticulum calcium pump expression during breast tumourigenesis. *Breast Cancer (Auckl)* 2011; 5: 163–74.
27. Dellis O, Arbabian A, Brouland JP, *et al*. Modulation of B-cell endoplasmic reticulum calcium homeostasis by Epstein-Barr virus latent membrane protein-1. *Mol Cancer* 2009; 8: 59.
28. Papp B, Brouland JP, Gélébart P, Kovàcs T, Chomienne C. Endoplasmic reticulum calcium transport ATPase expression during differentiation of colon cancer and leukaemia cells. *Biochem Biophys Res Commun* 2004; 322: 1223–36.
29. Gélébart P, Kovàcs T, Brouland JP, *et al*. Expression of endomembrane calcium pumps in colon and gastric cancer cells. Induction of SERCA3 expression during differentiation. *J Biol Chem* 2002; 277: 26310–20.
30. Launay S, Giannì M, Kovàcs T, *et al*. Lineage-specific modulation of calcium pump expression during myeloid differentiation. *Blood* 1999; 93: 4395–405.
31. Launay S, Bobe R, Lacabaratz-Porret C, *et al*. Modulation of endoplasmic reticulum calcium pump expression during T lymphocyte activation. *J Biol Chem* 1997; 272: 10746–50.
32. Wuytack F, Papp B, Verboomen H, *et al*. A sarco/endoplasmic reticulum $Ca^{(2+)}$-ATPase 3-type Ca^{2+} pump is expressed in platelets, in lymphoid cells, and in mast cells. *J Biol Chem* 1994; 269: 1410–6.
33. Papp B, Enyedi A, Pàszty K, *et al*. Simultaneous presence of two distinct endoplasmic-reticulum-type calcium-pump isoforms in human cells. Characterization by radio-immunoblotting and inhibition by 2,5-di-(t-butyl)-1,4-benzohydroquinone. *Biochem J* 1992; 288 (Pt 1): 297–302.
34. Papp B, Enyedi A, Kovàcs T, *et al*. Demonstration of two forms of calcium pumps by thapsigargin inhibition and radioimmunoblotting in platelet membrane vesicles. *J Biol Chem* 1991; 266: 14593–6.
35. Wuytack F, Dode L, Baba-Aissa F, Raeymaekers L. The SERCA3-type of organellar Ca^{2+} pumps. *Biosci Rep* 1995; 15: 299–306.
36. Arredouani A, Guiot Y, Jonas JC, *et al*. SERCA3 ablation does not impair insulin secretion but suggests distinct roles of different sarcoendoplasmic reticulum Ca(2+) pumps for Ca(2+) homeostasis in pancreatic beta-cells. *Diabetes* 2002; 51: 3245–53.
37. Chandrasekera PC, Kargacin ME, Deans JP, Lytton J. Determination of apparent calcium affinity for endogenously expressed human sarco(endo)plasmic reticulum calcium-ATPase isoform SERCA3. *Am J Physiol Cell Physiol* 2009; 296: C1105–14.
38. Rizzo FM, Palmirotta R, Marzullo A, *et al*. Parallelism of DOG1 expression with recurrence risk in gastrointestinal stromal tumours bearing KIT or PDGFRA mutations. *BMC Cancer* 2016; 16: 87.
39. Miettinen M, Wang ZF, Lasota J. DOG1 antibody in the differential diagnosis of gastrointestinal stromal tumours: a study of 1840 cases. *Am J Surg Pathol* 2009; 33: 1401–8.
40. Liegl B, Hornick JL, Corless CL, Fletcher CD. Monoclonal antibody DOG1.1 shows higher sensitivity than KIT in the diagnosis of gastrointestinal stromal tumours, including unusual subtypes. *Am J Surg Pathol* 2009; 33: 437–46.
41. Fletcher CD, Berman JJ, Corless C, *et al*. Diagnosis of gastrointestinal stromal tumours: a consensus approach. *Hum Pathol* 2002; 33: 459–65.
42. Hirota S, Isozaki K, Moriyama Y, *et al*. Gain-of-function mutations of c-kit in human gastrointestinal stromal tumours. *Science* 1998; 279: 577–80.
43. Sarlomo-Rikala M, Kovatich AJ, Barusevicius A, Miettinen M. CD117: a sensitive marker for gastrointestinal stromal tumours that is more specific than CD34. *Mod Pathol* 1998; 11: 728–34.
44. Antonescu CR, Romeo S, Zhang L, *et al*. Dedifferentiation in gastrointestinal stromal tumour to an anaplastic KIT-negative phenotype: a diagnostic pitfall: morphologic and molecular characterization of 8 cases occurring either de novo or after imatinib therapy. *Am J Surg Pathol* 2013; 37: 385–92.
45. Li L, Khalili M, Johannes G, *et al*. Case report of rhabdomyosarcomatous transformation of a primary gastrointestinal stromal tumour (GIST). *BMC Cancer* 2019; 19: 913.
46. Malik F, Santiago T, Bahrami A, *et al*. Dedifferentiation in SDH-deficient gastrointestinal stromal tumour: a report with histologic, immunophenotypic, and molecular characterization. *Pediatr Dev Pathol* 2019; 22: 492–8.
47. Medeiros F, Corless CL, Duensing A, *et al*. KIT-negative gastrointestinal stromal tumours: proof of concept and therapeutic implications. *Am J Surg Pathol* 2004; 28: 889–94.
48. Harhar M, Harouachi A, Akouh N, *et al*. Gastrointestinal stromal tumour in the fourth portion of the duodenum does not express the CD117: a case report. *Ann Med Surg (Lond)* 2022; 77: 103560.
49. Pantaleo MA, Urbini M, Schipani A, *et al*. SDHA germline variants in adult patients with SDHA-mutant gastrointestinal stromal tumour. *Front Oncol* 2021; 11: 778461.
50. Jansen K, Farahi N, Buscheck F, *et al*. DOG1 expression is common in human tumours: a tissue microarray study on more than 15,000 tissue samples. *Pathol Res Pract* 2021; 228: 153663.
51. Vallejo-Benitez A, Rodriguez-Zarco E, Carrasco SP, *et al*. Expression of dog1 in low-grade fibromyxoid sarcoma: a study of 19 cases and review of the literature. *Ann Diagn Pathol* 2017; 30: 8–11.
52. Miettinen M, Sobin LH, Sarlomo-Rikala M. Immunohistochemical spectrum of GISTs at different sites and their differential diagnosis with a reference to CD117 (KIT). *Mod Pathol* 2000; 13: 1134–42.
53. Miettinen M, Lasota J. KIT (CD117): a review on expression in normal and neoplastic tissues, and mutations and their clinicopathologic correlation. *Appl Immunohistochem Mol Morphol* 2005; 13: 205–20.
54. WHO Classification of Tumours Editorial Board. *WHO Classification of Tumours: Digestive System Tumours*. 5th ed. Lyon: IARC Press, 2019; 439–43.
55. Martini M, Santoro L, Familiari P, Costamagna G, Ricci R. Inflammatory fibroid polyp of the gallbladder bearing a platelet-derived growth factor receptor alpha mutation. *Arch Pathol Lab Med* 2013; 137: 721–4.
56. Ricci R, Arena V, Castri F. Role of p16/INK4a in gastrointestinal stromal tumour progression. *Am J Clin Pathol* 2004; 22: 35–43.
57. Yamamoto H, Oda Y, Kawaguchi K, *et al*. c-kit and PDGFRA mutations in extragastrointestinal stromal tumour (gastrointestinal stromal tumour of the soft tissue). *Am J Surg Pathol* 2004; 28: 479–88.
58. Pantaleo MA, Astolfi A, Urbini M, *et al*. Analysis of all subunits, SDHA, SDHB, SDHC, SDHD, of the succinate dehydrogenase complex in KIT/PDGFRA wild-type GIST. *Eur J Hum Genet* 2014; 22: 32–9.
59. Anger M, Samuel JL, Marotte F, Wuytack F, Rappaport L, Lompre AM. The sarco(endo)plasmic reticulum Ca(2+)-ATPase mRNA isoform, SERCA 3, is expressed in endothelial and epithelial cells in various organs. *FEBS Lett* 1993; 334: 45–8.
60. Wardelmann E, Hrychyk A, Merkelbach-Bruse S, *et al*. Association of platelet-derived growth factor receptor alpha mutations with gastric primary site and epithelioid or mixed cell morphology in gastrointestinal stromal tumours. *J Mol Diagn* 2004; 6: 197–204.
61. Lasota J, Dansonka-Mieszkowska A, Sobin LH, Miettinen M. A great majority of GISTs with PDGFRA mutations represent gastric tumours of low or no malignant potential. *Lab Invest* 2004; 84: 874–83.
62. Choi JJ, Sinada-Bottros L, Maker AV, Weisenberg E. Dedifferentiated gastrointestinal stromal tumour arising de novo from the small intestine. *Pathol Res Pract* 2014; 210: 264–6.
63. Desai J, Shankar S, Heinrich MC, *et al*. Clonal evolution of resistance to imatinib in patients with metastatic gastrointestinal stromal tumours. *Clin Cancer Res* 2007; 13: 5398–405.
64. Shankar S, vanSonnenberg E, Desai J, Dipiro PJ, Van Den Abbeele A, Demetri GD. Gastrointestinal stromal tumour: new nodule-within-a-mass pattern of recurrence after partial response to imatinib mesylate. *Radiology* 2005; 235: 892–8.
65. Chen H, Ordog T, Chen J, *et al*. Differential gene expression in functional classes of interstitial cells of Cajal in murine small intestine. *Physiol Genomics* 2007; 31: 492–509.
66. Nakayama S, Kajioka S, Goto K, Takaki M, Liu HN. Calcium-associated mechanisms in gut pacemaker activity. *J Cell Mol Med* 2007; 11: 958–68.
67. Dulin NO. Calcium-activated chloride channel ANO1/TMEM16A: regulation of expression and signaling. *Front Physiol* 2020; 11: 590262.
68. Drumm BT, Hwang SJ, Baker SA, Ward SM, Sanders KM. Ca(2+) signalling behaviours of intramuscular interstitial cells of Cajal in the murine colon. *J Physiol* 2019; 597: 3587–617.
69. Drumm BT, Rembetski BE, Huynh K, Nizar A, Baker SA, Sanders KM. Excitatory cholinergic responses in mouse colon intramuscular interstitial cells of Cajal are due to enhanced Ca(2+) release via M3 receptor activation. *FASEB J* 2020; 34: 10073–95.
70. Zheng H, Drumm BT, Earley S, Sung TS, Koh SD, Sanders KM. SOCE mediated by STIM and Orai is essential for pacemaker activity in the interstitial cells of Cajal in the gastrointestinal tract. *Sci Signal* 2018; 11: eaaq0918.
71. Baker SA, Drumm BT, Saur D, Hennig GW, Ward SM, Sanders KM. Spontaneous Ca(2+) transients in interstitial cells of Cajal located within the deep muscular plexus of the murine small intestine. *J Physiol* 2016; 594: 3317–38.
72. Drumm BT, Rembetski BE, Baker SA, Sanders KM. Tonic inhibition of murine proximal colon is due to nitrergic suppression of Ca(2+) signaling in interstitial cells of Cajal. *Sci Rep* 2019; 9: 4402.

73. Ward SM, Ordog T, Koh SD, *et al*. Pacemaking in interstitial cells of Cajal depends upon calcium handling by endoplasmic reticulum and mitochondria. *J Physiol* 2000; 525 (Pt 2): 355–61.
74. Baker SA, Leigh WA, Del Valle G, *et al*. Ca(2+) signaling driving pacemaker activity in submucosal interstitial cells of Cajal in the murine colon. *Elife* 2021; 10: e64099.
75. Drumm BT, Hennig GW, Battersby MJ, *et al*. Correction: clustering of Ca(2+) transients in interstitial cells of Cajal defines slow wave duration. *J Gen Physiol* 2017; 149: 751.
76. Drumm BT, Hennig GW, Battersby MJ, *et al*. Clustering of Ca(2+) transients in interstitial cells of Cajal defines slow wave duration. *J Gen Physiol* 2017; 149: 703–25.
77. Roskoski Jr R. Signaling by Kit protein-tyrosine kinase-the stem cell factor receptor. *Biochem Biophys Res Commun* 2005; 337: 1–13.
78. Roskoski Jr R. Structure and regulation of Kit protein-tyrosine kinase–the stem cell factor receptor. *Biochem Biophys Res Commun* 2005; 338: 1307–15.
79. Andrae J, Gallini R, Betsholtz C. Role of platelet-derived growth factors in physiology and medicine. *Genes Dev* 2008; 22: 1276–312.
80. Duensing A, Medeiros F, McConarty B, *et al*. Mechanisms of oncogenic KIT signal transduction in primary gastrointestinal stromal tumours (GISTs). *Oncogene* 2004; 23: 3999–4006.
81. Dode L, Vilsen B, Van Baelen K, Wuytack F, Clausen JD, Andersen JP. Dissection of the functional differences between sarco(endo)plasmic reticulum Ca^{2+}-ATPase (SERCA) 1 and 3 isoforms by steady-state and transient kinetic analyses. *J Biol Chem* 2002; 277: 45579–91.
82. Lytton J, Westlin M, Burk SE, Shull GE, MacLennan DH. Functional comparisons between isoforms of the sarcoplasmic or endoplasmic reticulum family of calcium pumps. *J Biol Chem* 1992; 267: 14483–9.
83. Vandecaetsbeek I, Trekels M, De Maeyer M, *et al*. Structural basis for the high Ca^{2+} affinity of the ubiquitous SERCA2b Ca^{2+} pump. *Proc Natl Acad Sci USA* 2009; 106: 18533–8.
84. Kovàcs T, Felföldi F, Papp B, *et al*. All three splice variants of the human sarco/endoplasmic reticulum Ca^{2+}-ATPase 3 gene are translated to proteins: a study of their co-expression in platelets and lymphoid cells. *Biochem J* 2001; 358: 559–68.
85. Martin V, Bredoux R, Corvazier E, Papp B, Enouf J. Platelet Ca(2+) ATPases : a plural, species-specific, and multiple hypertension-regulated expression system. *Hypertension* 2000; 35: 91–102.
86. Baba-Aissa F, Raeymaekers L, Wuytack F, Dode L, Casteels R. Distribution and isoform diversity of the organellar Ca^{2+} pumps in the brain. *Mol Chem Neuropathol* 1998; 33: 199–208.
87. Elaib Z, Adam F, Berrou E, *et al*. Full activation of mouse platelets requires ADP secretion regulated by SERCA3 ATPase-dependent calcium stores. *Blood* 2016; 128: 1129–38.
88. Feng M, Elaib Z, Borgel D, *et al*. NAADP/SERCA3-dependent Ca(2+) stores pathway specifically controls early autocrine ADP secretion potentiating platelet activation. *Circ Res* 2020; 127: e166–83.
89. Wang Y, Marino-Enriquez A, Bennett RR, *et al*. Dystrophin is a tumour suppressor in human cancers with myogenic programs. *Nat Genet* 2014; 46: 601–6.
90. Barrett T, Wilhite SE, Ledoux P, *et al*. NCBI GEO: archive for functional genomics data sets-update. *Nucleic Acids Res* 2013; 41: D991–5.
91. Edgar R, Domrachev M, Lash AE. Gene expression omnibus: NCBI gene expression and hybridization array data repository. *Nucleic Acids Res* 2002; 30: 207–10.
92. Detwiller KY, Fernando NT, Segal NH, Ryeom SW, D'Amore PA, Yoon SS. Analysis of hypoxia-related gene expression in sarcomas and effect of hypoxia on RNA interference of vascular endothelial cell growth factor A. *Cancer Res* 2005; 65: 5881–9.
93. Yoon SS, Segal NH, Park PJ, *et al*. Angiogenic profile of soft tissue sarcomas based on analysis of circulating factors and microarray gene expression. *J Surg Res* 2006; 135: 282–90.
94. Liegl B, Hornick JL, Antonescu CR, Corless CL, Fletcher CD. Rhabdomyosarcomatous differentiation in gastrointestinal stromal tumours after tyrosine kinase inhibitor therapy: a novel form of tumour progression. *Am J Surg Pathol* 2009; 33: 218–26.
95. Karakas C, Christensen P, Baek D, Jung M, Ro JY. Dedifferentiated gastrointestinal stromal tumour: recent advances. *Ann Diagn Pathol* 2019; 39: 118–24.
96. Wardelmann E, Merkelbach-Bruse S, Pauls K, *et al*. Polyclonal evolution of multiple secondary KIT mutations in gastrointestinal stromal tumours under treatment with imatinib mesylate. *Clin Cancer Res* 2006; 12: 1743–9.
97. Ricci R, Giustiniani MC, Gessi M, *et al*. Telocytes are the physiological counterpart of inflammatory fibroid polyps and PDGFRA-mutant GISTs. *J Cell Mol Med* 2018; 22: 4856–62.
98. Sanders KM, Ward SM, Koh SD. Interstitial cells: regulators of smooth muscle function. *Physiol Rev* 2014; 94: 859–907.
99. Kurahashi M, Mutafova-Yambolieva V, Koh SD, Sanders KM. Platelet-derived growth factor receptor-alpha-positive cells and not smooth muscle cells mediate purinergic hyperpolarization in murine colonic muscles. *Am J Physiol Cell Physiol* 2014; 307: C561–70.
100. Bardsley MR, Horvàth VJ, Asuzu DT, *et al*. Kit^{low} stem cells cause resistance to Kit/platelet-derived growth factor alpha inhibitors in murine gastrointestinal stromal tumours. *Gastroenterology* 2010; 139: 942–52.
101. Banerjee S, Yoon H, Ting S, *et al*. KIT(low) cells mediate imatinib resistance in gastrointestinal stromal tumour. *Mol Cancer Ther* 2021; 20: 2035–48.
102. Subramanian S, West RB, Corless CL, *et al*. Gastrointestinal stromal tumours (GISTs) with KIT and PDGFRA mutations have distinct gene expression profiles. *Oncogene* 2004; 23: 7780–90.
103. Sapi Z, Füle T, Hajdù M, *et al*. The activated targets of mTOR signaling pathway are characteristic for PDGFRA mutant and wild-type rather than KIT mutant GISTs. *Diagn Mol Pathol* 2011; 20: 22–33.
104. Corless CL, Schroeder A, Griffith D, *et al*. PDGFRA mutations in gastrointestinal stromal tumours: frequency, spectrum and *in vitro* sensitivity to imatinib. *J Clin Oncol* 2005; 23: 5357–64.